Applied Catalysis B: Environment and Energy 353 (2024) 124075

Contents lists available at ScienceDirect

Applied Catalysis B: Environment and Energy

journal homepage: www.elsevier.com/locate/apcatb

Mechanistic insight into the mutual-effect and key intermediate during methanol accelerating toluene decomposition over Co-spinel catalyst revealed by PTR-TOF-MS and DFT calculation

Jinping Zhong [a,c,1], Zheng Yin [b,1], Tan Li [c,1], Yikui Zeng [a], Fada Feng [a], Quanming Ren [c], Dengfeng Yan [c], Tao Dong [d], Yuanyuan Meng [e], Haibao Huang [d,*], Daiqi Ye [c,*]

[a] School of Chemistry and Environment, Jiaying University, Meizhou, China
[b] School of Chemistry and Pharmaceutical Sciences, State Key Laboratory for Chemistry and Molecular Engineering of Medicinal Resources, Guangxi Normal University, Guilin, China
[c] School of Environment and Energy, South China University of Technology, Guangzhou, China
[d] School of Environmental Science and Engineering, Sun Yat-Sen University, Guangzhou, China
[e] College of Chemistry and Chemical Engineering, Taiyuan University of Technology, Taiyuan, China

ARTICLE INFO

Keywords:
VOCs
Co-spinel
Mutual-effect
Intermediate
Mechanism

ABSTRACT

Revealing the inherent mechanism of multi-component VOCs paves the way for the development of new efficient catalysts applicable to the practical elimination of VOCs. For two primary co-existing industry VOCs of toluene and methanol, their synergetic and efficient oxidation are investigated based on two Co_3O_4 catalysts with exposed {111} and {110} faces. The promoting effect of methanol on toluene oxidation, with a significant decrease in conversion temperature compared to that of toluene alone, has experimentally and theoretically identified for the first time. The formaldehyde produced by methanol oxidation reacts with toluene to form 2-methylbenzaldehyde as a key intermediate, leading to a lower energy barrier in the aromatic-ring-opening of toluene during the oxidation path. The intrinsically higher conversion temperature of toluene than methanol synchronously guarantees the full decomposition of methanol. This work sheds light on a new insight into the reaction mechanism of the mutual-effect produced by multi-component VOC oxidation.

1. Introduction

High-efficient elimination technology is urgently needed due to the serious threat of volatile organic compounds (VOCs) to human health and ecosystems. Catalytic oxidation is considered to be the first choice for the transformation of VOCs into carbon dioxide and water with high efficiency and economic feasibility [1]. At present, there have been a good advance in the single-component catalytic oxidation of toluene, methanol, acetone, formaldehyde, ethyl acetate, and others [2–6]. However, various VOCs often coexist in realistic environments, given that they were generated from similar industrial sources [4,5]. The mixed VOC contaminants have been widely found in several important industries like plastic, dyeing, printing, pharmaceuticals, and fine chemicals [2,5,7]. Obviously, studying the catalytic oxidation of single VOC components is difficult to meet the practical needs of full VOC treatment in an actual environment. The catalytic activity and the inherent oxidation mechanism of different types of VOCs are quite different. It is still unclear whether the high catalytic efficiency of certain catalysts for a single component is maintained in mixed VOCs, considering the diversiform intermediates and their inevitable effects on catalytic performance. Therefore, it is of great practical significance to study the relevance and mutual-effect between the different oxidation paths of coexisting VOCs and estimate the overall VOC decomposition performance of a selected catalyst.

Indeed, though quite rare, promotion or inhibition effects have been occasionally found when different VOCs coexist in a handful of studies [5,8–13]. Recently, Deng et al. have found that the mixing of toluene and acetone leads to reduced catalysis efficiency on Pt/TiO_2 of both the VOCs because of the mutual competition in surface adsorption between the reaction molecules [14]. Santos et al. also noticed that ethyl acetate

* Corresponding authors.
E-mail addresses: huanghb6@mail.sysu.edu.cn (H. Huang), cedqye@scut.edu.cn (D. Ye).
[1] These authors contributed equally.

https://doi.org/10.1016/j.apcatb.2024.124075
Received 19 December 2023; Received in revised form 2 April 2024; Accepted 13 April 2024
Available online 16 April 2024

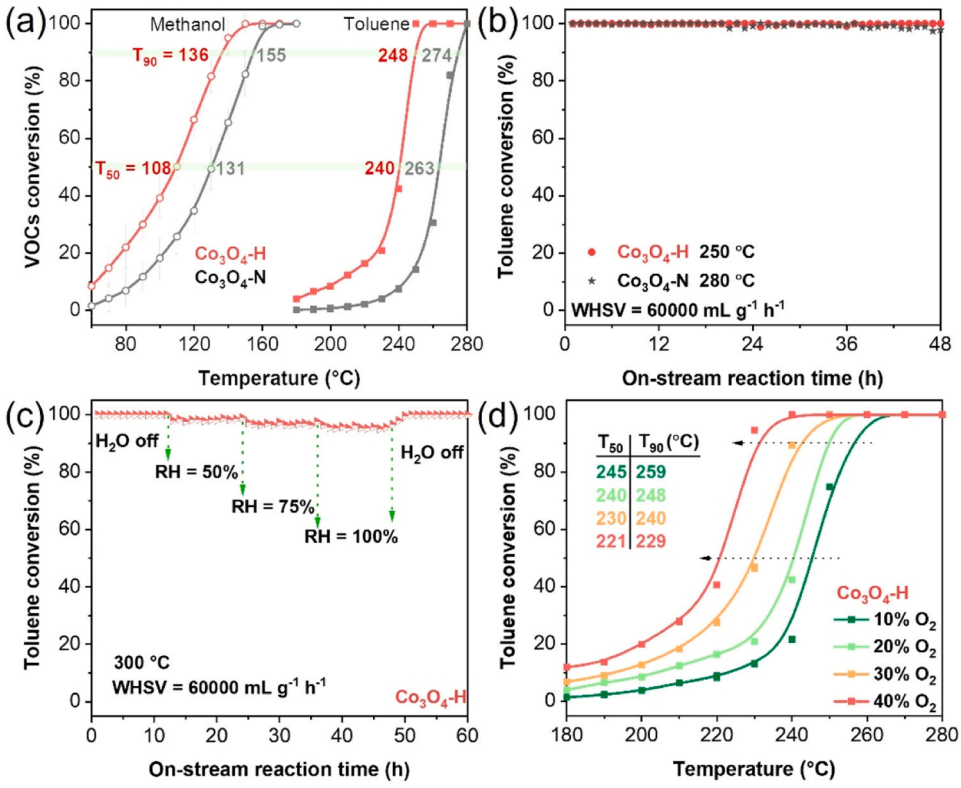

Fig. 1. The temperature dependent conversion of (a) toluene and methanol over the Co_3O_4 catalysts. (b) The time dependent conversion stability for toluene up to 48 h. (c) The effect of water vapor with different RH on toluene oxidation over Co_3O_4-H. (d) The conversion of toluene over Co_3O_4-H under different oxygen concentrations.

restrains the oxidation of toluene using cryptomelane as a catalyst [15]. In contrast, He et al., found that ethyl acetate has a favorable promoting effect for toluene oxidation on Pd/ZSM-5 catalyst [16]. However, due to the lack of crucial experimental evidence, the synergetic process and mechanism are unclear for these interesting findings, only inferring to the competitive adsorption or thermal effect of the reactant on the catalyst surface. Apparently, compared with the inherent mechanism and reaction path of single-component VOCs on the applied catalyst. Multi-component VOC systems involve quite complex intermediates, different stability and chemical reactivity, competitive adsorption on the surface, and catalytic sites, which lead to rich mutual-effects among different VOCs. Nevertheless, the current research only simply attributes the catalytic promotion or inhibition of different components to the influence of local thermal effects or competitive adsorption on surface, etc., which is inadequate due to missing in identification of key intermediates. Moreover, a series of parameters on reaction conditions and catalyst structure are potentially relevant to the cause of the mutual influence of coexisting VOCs, making the mechanism complex and unclear [17]. Hence, it is essential to systematically study and understand the inherent mechanism of co-catalytic oxidation in multi-component VOC systems from a molecular level, driven by the great potential of practical environmental remediation.

On this occasion, the mixture of toluene and methanol comes into our sight, considering their widespread coexistence, high concentration in industry, and great hazards to humans [5,18,19]. Especially, the efficient elimination of toluene is challenging due to the high conversion temperature needed to break the conjugated aromatic ring as well as catalyst poisoning stemming from the deposition of high-content carbon. Considering the much lower conversion temperature and lower carbon ratio of methanol, the synergistic effect makes it interesting to explore the energy-efficient and full elimination of mixed VOCs of methanol and toluene. In our previous work, we used a gentle hydrolysis of 1D nanowire MOF to prepare a good VOC catalyst, namely hydrangea-like Co_3O_4-H and nanowire shaped Co_3O_4-N [20]. They exhibited significant enhanced catalytic performance for toluene degradation and benefited from rich oxygen vacancies on the exposed facet. These two catalysts provide quite suitable candidates to investigate the mutual-effects of coexisting VOCs and their inherent reaction mechanisms related to the exposed crystal facet, activation site, intermediate, and reaction paths. Here, we endeavor to comprehensively explore the mutual-effect of catalytic oxidization between toluene and methanol. The promoting effect of methanol on toluene oxidation, with a significant decrease in T_{50} of 32 °C and T_{90} of 23 °C compared to that of toluene alone, are experimentally and theoretically identified. The insight into the inherent mechanism was supported by a systematic characterization including VOCs temperature program surface reaction (VOCs-TPSR), in-situ diffused reflectance infrared Fourier transform spectroscopy (in-situ DRIFTS), Proton Transfer Reaction-Time of Flight-Mass Spectrometer (PTR-TOF-MS) as well as Density Functional Theory (DFT) calculation. This work provides us a new mechanism insight into the mutual-effect generating from multi-component VOC oxidation.

2. Experimental section

2.1. Experimental and characterization

Synthesis of tricobalt tetroxide nanowires (Co_3O_4-N): the synthesis of nanowires like (Co_3O_4-N) is based on the previously reported [20]. In a typical process, 1.77 mmol of the cobalt tetrahydrate is dissolved in 60 mL of methanol, followed by adding 6.1 mmol of 2,5-dihydroxyterephthalic acid (DHT). The resulting mixture is further ultrasonicated for 10 min and then centrifuged. The obtained precipitate is washed by methanol and distilled water several times to remove the unreacted compositions for further use, denoted as Co-MOF-74 nanowires. The as-prepared Co-MOF-74 nanowires is transferred into a ceramic boat

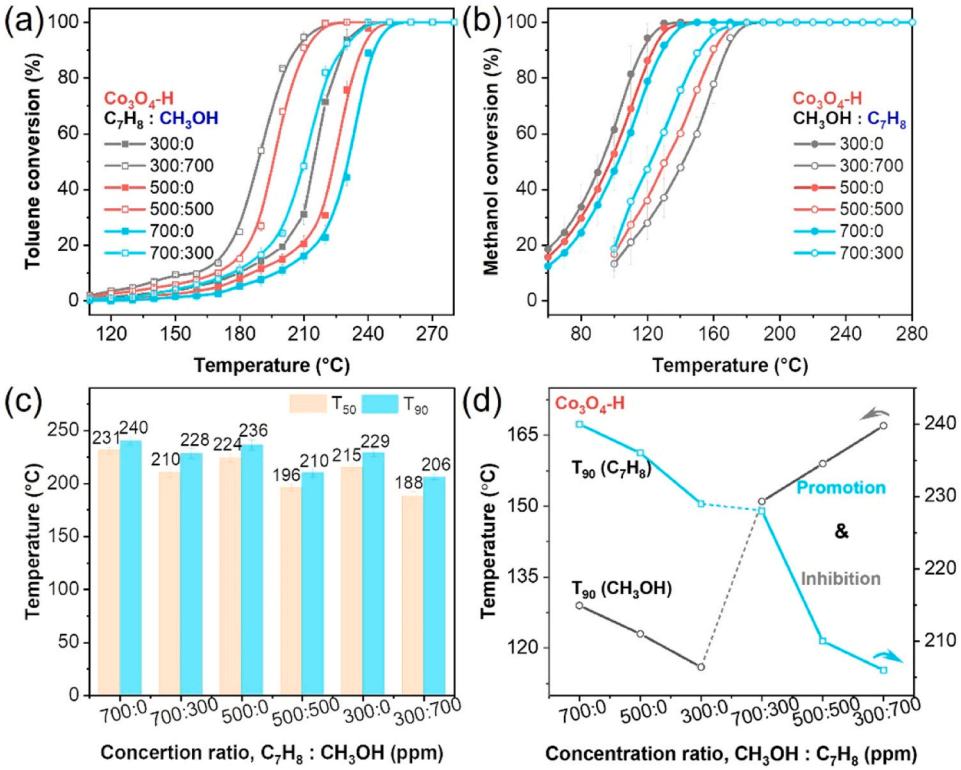

Fig. 2. The oxidation performance of (a) toluene and (b) methanol over the Co_3O_4-H under different VOCs ratios. (c) The T_{50} and T_{90} values for methanol and toluene oxidation. (d) The T_{90} conversion trend diagram of methanol and toluene in single and two components. Reaction conditions: x ppm methanol + y ppm toluene (x + y = 1000, x = 300, 500, and 700), the total flow rate = 100 mL·min^{-1}, WHSV = 60000 mL·g^{-1}·h^{-1}.

and placed in a tube furnace under an O_2 flow. They are heated up to 350 °C at a rate of 1 °C/min and maintained at this temperature for 3.5 h to obtain the tricobalt tetroxide nanowires, denoted as Co_3O_4-N.

Synthesis of hydrangeas like tricobalt tetroxide (Co_3O_4-H): The precursors of Co-MOF-74 are dispersed in 60 mL of distilled water, followed by the addition amount of 4.2 mmol of urea. The mixture is then transferred into a 100 mL Teflon-lined autoclave and placed in an oven at 140 °C for 24 h. After cooling down to room temperature, the obtained precipitate is centrifugally washed with distilled water and ethanol to obtain the purple hydrangea structure (denoted as $CoCO_3$-H). Then the $CoCO_3$-H is calcined in the same process to obtain hydrangea like tricobalt tetroxide, denoted as Co_3O_4-H.

The as-obtained catalysts are characterized by catalysts was investigated by scanning electron microscopy (SEM), Powder X-ray diffraction (PXRD), electron paramagnetic resonance (EPR), volatile organic compounds temperature programmed surface reaction (VOCs-TPSR), and in situ diffuse reflection infrared Fourier transform spectroscopy (in-situ DRIFTS) as well as the Proton Transfer Reaction-Time of Flight-Mass (PTR-TOF-MS). For more details on the synthetic process and characterization experiments, please refer to the Supporting Information.

2.2. Catalytic evaluation and computational methods

For detailed catalytic evaluation and computational methods, please refer to the Supporting Information.

3. Results and discussions

3.1. Structure characterization

The apparent morphology of the catalysts was investigated by SEM and HRTEM. As shown in Fig. S1 and S2, the synthesized Co_3O_4-H and Co_3O_4-N exhibit hydrangea and nanowire morphologies, and mainly exposed the {110} and {111} facets, respectively. The PXRD patterns of the fabricated catalysts are consistent with those of the cube-phase spinel Co_3O_4 (PDF No. 42–1476) (Fig. S3). Both samples exhibited a symmetrical EPR peak at the *g* value of 2.00 (Fig. S4), stemming from the free electrons trapped in the oxygen vacancies [21]. The peak intensity of Co_3O_4-H is much greater than that of Co_3O_4-N, indicating more oxygen vacancy defects in Co_3O_4-H [22].

3.2. Catalytic performance

The isolated toluene and methanol degradation over the Co-based catalysts was first investigated to estimate their catalytic behaviors as a criterion (Fig. 1 and Table S1). The catalytic oxidation activity of Co_3O_4-H for both toluene and methanol are higher than that of Co_3O_4-N, indicating the positive correlation of more oxygen vacancy defects with promoted catalytic degradation efficiency. The measured T_{90} values for toluene and methanol conversion over Co_3O_4-H are 248 and 136 °C, respectively. In addition, the Co_3O_4-H at 250 °C and Co_3O_4-N at 280 °C can well maintain 100% conversion for toluene oxidation up to 48 h (Fig. 1b) at a WHSV of 60000 mL·g^{-1}·h^{-1}. Considering the inevitable influence of water vapor in practical environments, the catalytic efficiency of Co_3O_4-H on toluene oxidation under different relative humidity (RH) was investigated at a reaction temperature of 300 °C. Even at an extremely high humidity of 100%, the Co_3O_4-H can maintain a high conversion of 96% (Fig. 1c). When the addition of water vapor stopped, the degradation of toluene quickly recovered to 100%. These results well confirm the good moisture resistance of Co_3O_4-H as a catalyst suitable for an actual atmosphere with varying humidity. Furthermore, the higher oxygen concentration imposes a promoting effect on the degradation of toluene, giving a decreased T_{90} of 229 °C at an oxygen concentration of 40% for Co_3O_4-H (Fig. 1d). The reason for this might be to that more oxygen vacancies favor to adsorb and activate oxygen species.

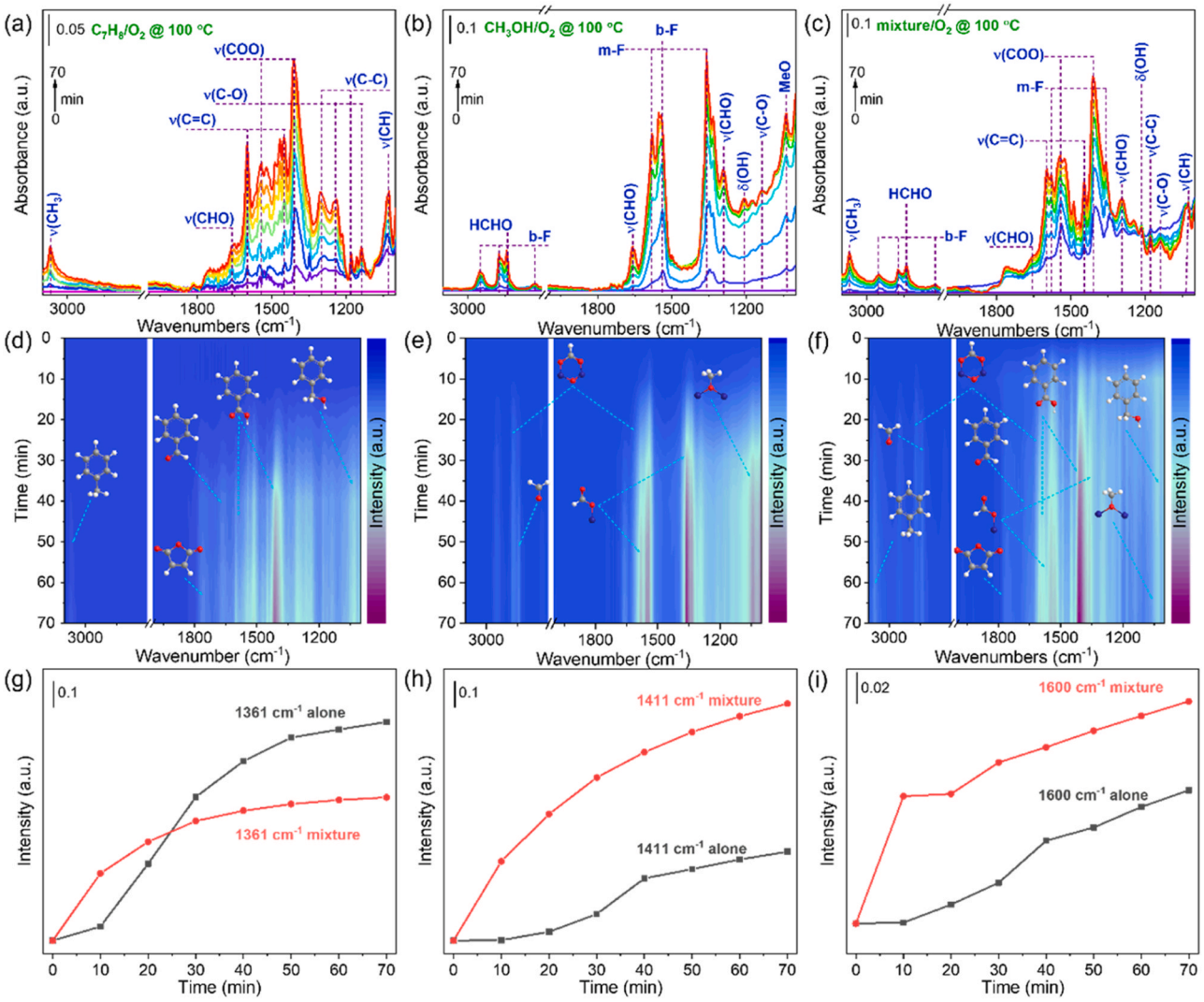

Fig. 3. In-situ DRIFTS spectra (up) and corresponding contour colour maps (middle) of the transient reactions of (a, d) toluene, (b, e) methanol, and (c, f) the mixture of methanol and toluene over the Co_3O_4-H catalyst at 100 °C as a function of time;(g-i) Plots of normalized intensities of typical characteristic peaks of mono-dentate formate species (1361 cm^{-1}), benzoate species (1411 cm^{-1}), and benzaldehyde species (1600 cm^{-1}) alone and in mixture versus reaction time, respectively.

As is known to all, during the catalytic oxidation of VOCs on transition metal oxides, the formation of oxygen vacancies and oxygen supplementation on the metal oxides were considered to be determinants of their catalytic performance [23]. Thus, the oxygen vacancy formation energy over these two Co_3O_4 catalysts was calculated (Fig. S5). For Co_3O_4-N, the oxygen vacancy formation energies for O_a and O_b are 3.44 and 3.12 eV, respectively. While for Co_3O_4-H, the oxygen vacancy formation energies for O_a' and O_b' are 0.84 and 0.36 eV, respectively. These results suggested that Co_3O_4-H with a mainly exposed {110} facet made it easier to form oxygen vacancies, which is in accordance with EPR analysis. In addition, the adsorption energy of gaseous oxygen on the above oxygen vacancy was calculated, as illustrated in Fig. S6. The adsorption energies of Co_3O_4-H for O_a and O_b are −0.91 and −0.49 eV, respectively, which are lower than those of the Co_3O_4 {111} facet (-0.11 and 2.31 eV) (Fig. S6a and b). It is revealed that the adsorption of oxygen molecules on Co_3O_4 {110} is easier than that on the Co_3O_4 {111} facet. Therefore, compared with Co_3O_4-N, the oxygen vacancy on the surface of Co_3O_4-H is more likely to form and be supplemented by molecular oxygen, which accelerates the cycle of oxygen species in the reaction process and thus improves its catalytic activity for toluene and methanol.

To reveal the mutual-effect of mixed VOC components, methanol with different concentrations was introduced to study the synergetic catalytic oxidation of toluene over Co_3O_4-H (Fig. 2 and Table S1). Interestingly, with the increase in methanol concentration (300, 500, and 700 ppm), the toluene oxidation temperature became significantly lower. Especially when 500 ppm methanol and 500 ppm toluene coexisted, the promotion of methanol to the oxidation of toluene is the most significant. The T_{50} and T_{90} of toluene oxidation over the Co_3O_4-H catalyst are 196 and 210 °C, respectively, which are 28 and 26 °C lower than those of 500 ppm toluene alone (Fig. 2a and c). This T_{90} value of toluene is outstanding in known 3D-metal VOC catalysis and comparable to those of precious metal catalysts that were summarized in Table S2. In turn, the conversion of methanol oxidation slightly shifted to a higher temperature region than that of methanol alone. The T_{50} and T_{90} of methanol oxidation over the Co_3O_4-H catalyst were 142 and 167 °C, respectively, for the reactant mixture of 300 ppm methanol and 700 ppm toluene (Fig. 2b). The reaction trend of T_{90} for methanol and toluene is shown in Fig. 2d. This methanol conversion temperature is much lower than that of toluene, suggesting that the decomposition of toluene simultaneously leads to the full elimination of methanol. The results of the above activity analyses preliminarily indicate that during the co-oxidation of methanol and toluene, methanol promotes the catalytic degradation of toluene, while toluene inhibits the catalytic

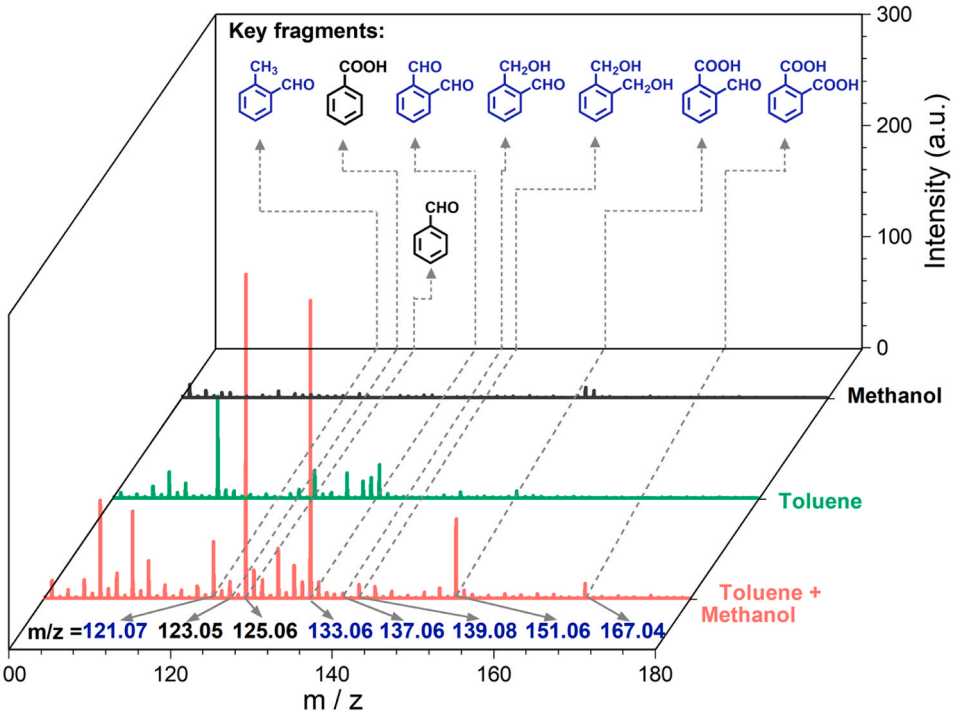

Fig. 4. PTR-TOF-MS spectra in m/z = 100–180 for toluene, methanol and their mixture under oxygen as carrier gas.

oxidation of methanol.

In order to make clear the inherent mechanism of the catalytic degradation involving mixed toluene and methanol, a series of experiments and theoretical calculations were performed. The subsequent TPSR profiles of toluene, methanol, and their mixtures (toluene + methanol) over Co_3O_4-H were first collected (Fig. S7). It is worth noting that the desorption peak temperature of CO_2 in the TPSR of the toluene-methanol mixture was 201 °C, which is lower than that of the toluene-TPSR with a desorption temperature of 223 °C and higher than that of the methanol-TPSR with a desorption temperature of 178 °C. Furthermore, the desorption temperature of toluene for the mixture-TPSR (75 °C) is lower than that of toluene-TPSR alone (89 °C). The desorption temperature of methanol for the mixture-TPSR (143 °C) is higher than that of methanol-TPSR alone (129 °C). These preliminary findings indicated that the coexistence of toluene and methanol altered their corresponding activation and oxidation processes.

3.3. Co-oxidation reaction mechanism

To further reveal the reaction mechanism of the co-oxidation of toluene and methanol over Co_3O_4-H, in-situ DRIFTS is performed to track the changes of intermediate species, and the results are illustrated in Fig. 3 and summarized in Table S3. When the Co_3O_4-H catalyst is exposed to 200 ppm toluene/air at 100 °C, the peak around 3068 cm^{-1} is attributed to the ν(C-H) vibration of the methyl group (CH_3) (Fig. 3a and d) [24]. The stronger peaks around 1540, 1411, and 1135 cm^{-1} are assigned to the asymmetric (COO) and symmetric vibrations of the carboxylate (-COO-) group [25], suggesting that the benzoate species are the key intermediates for toluene oxidation. The peak at about 1660 cm^{-1} is associated with the ν(C═O) aldehyde [1,3], indicating the formation of benzaldehyde species. The peaks around the 1600, 1513, and 1448 cm^{-1} are corresponded to the typical skeletal ν(C═C) vibration of toluene [14]. The peaks at 1303, 1180, and 1025 cm^{-1} are associated with benzyl alcohol [26]. The peaks around the 1760–2000 cm^{-1} region and 1238 cm^{-1} are attributed to the maleic anhydride [24,27]. In view of the above analysis and previous literature reports [24,28], the reaction process of toluene oxidation may follow the following pathway: toluene → benzyl alcohol → benzaldehyde → benzoic acid, and then ring-opened products of maleic acid to the final products of carbon dioxide and water. As a comparison, there are four peaks around 2950, 2873, 2726, and 1542 cm^{-1} attributed to the bi-dentate formate (b-F) from the in-situ DRIFTS results of methanol degradation (Fig. 3b and e) [6,29]. The intensity of the peaks around 2842, 1658, and 1292 cm^{-1} increased with the extension of the reaction time, indicating the accumulation of formaldehyde species [29,30]. The peaks around 1581 and 1361 cm^{-1} are assigned to the mono-dentate formate species (m-F) of ν_{as}(OCO) [31]. The peaks around the 1211, 1137, and 1037 cm^{-1} are correspond to the vibration of δ(OH), ν(C-O), and the methoxy group (MeO) bridge adsorbed on oxygen vacancies [6, 32]. Based on the above analytical experiments and in conjunction with previous works [13,33], the oxidation procedure of methanol might have the sequences of methanol → formaldehyde → formic acid, and finally carbon dioxide and water.

No new intermediate species was observed during the oxidation process of methanol and toluene mixtures (Fig. 3c and f), compared to the catalytic oxidation of methanol or toluene alone. For better analysis, the normalized band intensities of the characteristic peaks of key species of mono-dentate formate, benzoate, and benzaldehyde are plotted as a function of reaction time (Fig. 3g-i). It is found that the intensity of the typical adsorption peak of mono-dentate formate species (1361 cm^{-1}) in the mixture of toluene and methanol is significantly lower than that of methanol alone (Fig. 3g). While the typical characteristic peak of benzoate (1411 cm^{-1}) in Fig. 3h and benzaldehyde species (1600 cm^{-1}) in Fig. 3i under mixed conditions was significantly stronger than that of toluene alone. These results demonstrated that the coexistence of toluene and methanol is not conducive to the conversion of methanol to formate species but promotes the conversion of toluene to benzaldehyde, and benzoate species. Therefore, the conversion of toluene to benzaldehyde, benzoate and the conversion of methanol to formaldehyde and formic species are the key steps in the process of the co-oxidation of toluene and methanol.

In view of the above findings, we propose the following hypotheses about the promotion effect: Firstly, under the coexistence of methanol and toluene, the methanol adsorbed on the catalyst surface will be

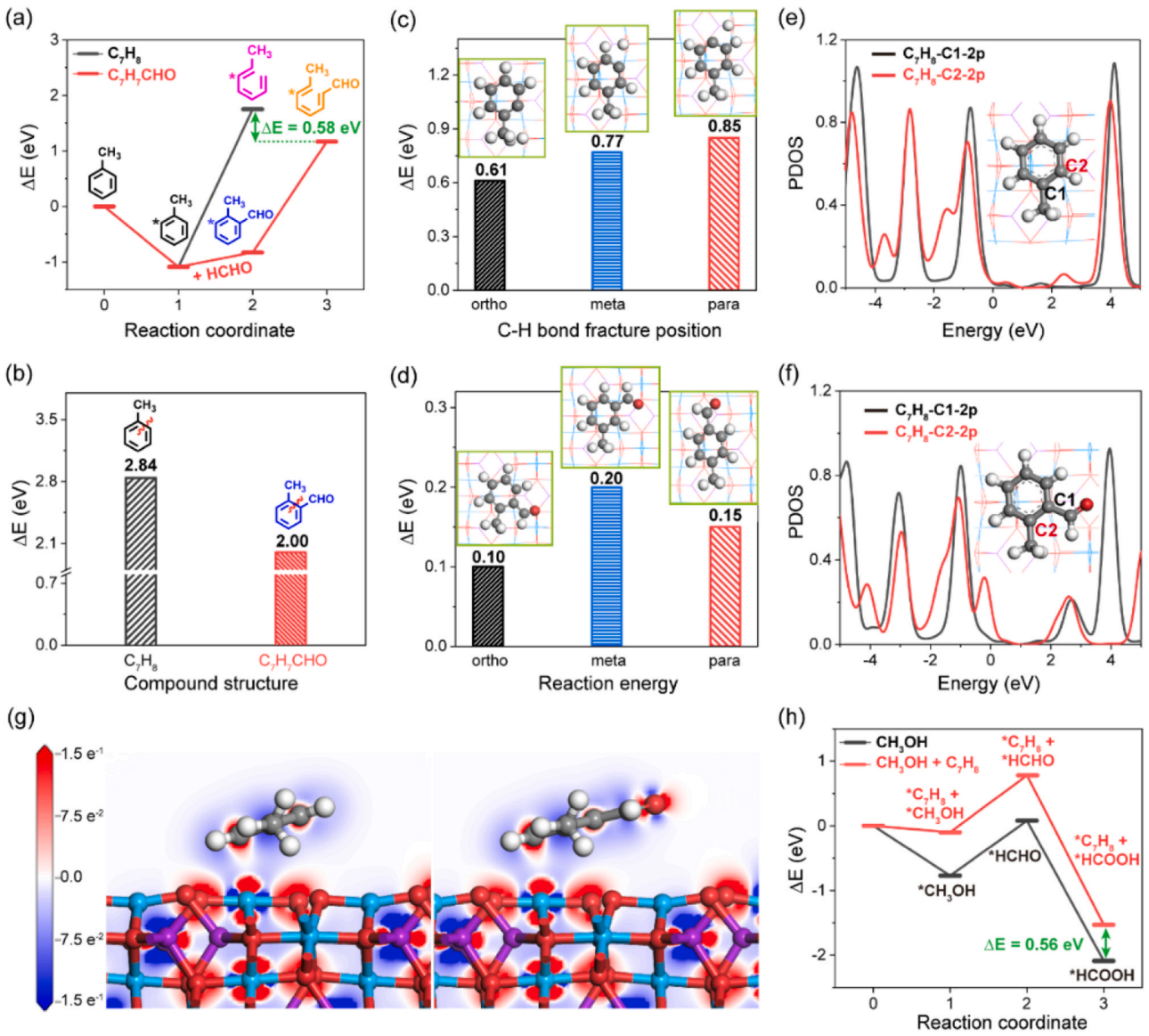

Fig. 5. DFT calculations for reaction mechanism analysis: (a) diagram of reaction energy (ΔE) variation and (b) C-H bond breaking energy for toluene (C_7H_8) and 2-methylbenzaldehyde (C_7H_7CHO) over {110} facet; (c) C-H bond fracture energy with different position; (d) the reaction energy of formaldehyde grafted on ortho, meta and para positions of toluene; projected density of states (PDOS) calculations for toluene (e) and 2-methylbenzaldehyde (f); (g) electron density differences (EDD) of toluene (left) and 2-methylbenzaldehyde (right) adsorbed on Co_3O_4-H catalyst. Note: The red and blue colours represent electron rich and deficient areas, respectively. (h) The reaction energy profile for the most representative paths way of methanol converted to formate species in the co-existence of methanol and toluene (red line) and methanol alone (dark line).

oxidized to form a formaldehyde intermediate at a lower temperature. Then the formation of formaldehyde and the adsorbed toluene will undergo substitution reactions to form the methylbenzaldehyde intermediate. Given that the DRIFTS technique mainly detects the substances adsorbed on the catalyst surface [8], PTR-TOF-MS was hence applied to find key intermediates from the gas-phase reaction process and further validate our hypothesis. The main information about by-product species is summarized in Table S4 and illustrated in Fig. S8-10. Within the mass charge ratio (m/z) in the range of 100–180 (Fig. 4), the m/z at 121.07 is attributed to the key intermedia of 2-methylbenzaldehyde, and the m/z at 133.06, 137.06, 139.08, 151.06, and 167.04 can be summed up the o-phthalaldehyde with removal of one H [34], 2-hydroxymethylbenzaldehyde, 1,2-phenylenedimethanol, 2-carboxybenzaldehyde, and phthalic acid, respectively. It is worth noting that the above characteristic peaks also appear during the catalytic oxidation of toluene alone. A reasonable explanation is that the catalytic oxidation process of toluene is always accompanied by the presence of a small amount of methanol, formaldehyde, and other molecules, which have been well verified in the previous work [24,35]. These concomitants of methanol or formaldehyde will inevitably react with toluene to generate products such as 2-methylbenzaldehyde species. However, the relative concentration of these products is significantly lower than that observed from methanol and toluene in the mixture. As a comparison, the single catalytic oxidation of methanol did not generate these products. In addition, the peak of $m/z = 123.05$ could be assigned to the benzoic acid, and $m/z = 125.06$ can be attributed to the benzaldehyde. The intensity of these two peaks from a mixture of methanol and toluene was stronger than that of toluene alone, which was in accordance with the in-situ DRIFTS analysis. Hence, the formaldehyde generated by the oxidation of methanol would first react with toluene to form the key intermediate 2-methylbenzaldehyde during the co-oxidation of toluene and methanol, which plays the role of a key knob that leads to the promoted oxidation of toluene.

The DFT calculation was further performed to confirm the role of the key intermediate, 2-methylbenzaldehyde. The calculated reaction

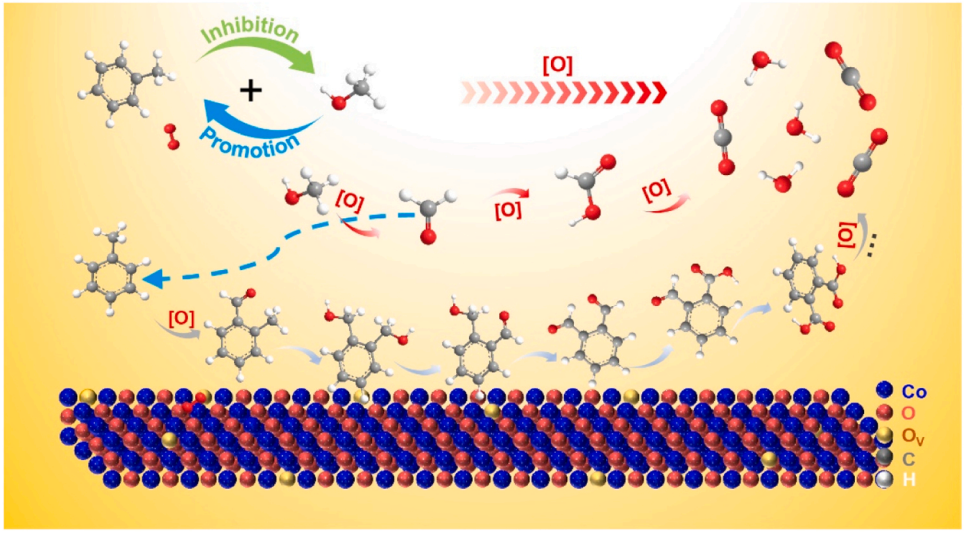

Scheme 1. Proposed mechanism for the co-oxidation of toluene and methanol over Co_3O_4 catalyst.

energy of toluene is higher by about 0.58 eV than that of 2-methylbenzaldehyde (Fig. 5a). It is well known that ring-opening is the bottleneck and rate-controlled step for the degradation of aromatic ring compounds [3,8,26,36]. Therefore, the bond-breaking energies of toluene and 2-methylbenzaldehyde are calculated separately. The bond breaking energy (2.84 eV) for toluene is higher than that of 2.00 eV for 2-methylbenzaldehyde (Fig. 5b and Fig. S11), indicating the aromatic ring of 2-methylbenzaldehyde is preferential to opening. The optimal DFT structures of toluene adsorbed on the {110} facet was further confirmed (Fig. S12), which exhibited the lowest adsorption energy absorbed on α. In order to confirm the structure of the key intermediate 2-methylbenzaldehyde, the fracture energy of C-H at the ortho (o), meta (m), and para (p) positions of toluene and the formation energy of o-, m-, and p-methylbenzaldehyde grafted by formaldehyde on the o-, m- and p-positions of toluene are calculated (Fig. 5c-d and Fig. S13-14). The reaction energy required for the activation of the C-H bond in the o-position of toluene is the lowest (0.61 eV), followed by the m- position (0.77 eV) and p-positions (0.85 eV). The formation energy of o-methylbenzaldehyde is the lowest (0.10 eV), followed by p-methylbenzaldehyde (0.15 eV) and m-methylbenzaldehyde (0.20 eV). Similarly, there is the possibility to form the isomers of o-methylbenzaldehyde and phenylethlaldehyde, for which the formation energy and the energy barrier required for ring opening are calculated (Fig. S15). As a result, in the process of the co-oxidation of toluene and methanol, formaldehyde is quite facile to react with the C-H of toluene at o-position to form the more stable 2-methylbenzaldehyde.

Furthermore, the electronic structures of toluene and 2-methylbenzaldehyde on the catalyst surface were analyzed. The results of the projected density of states (PDOS) calculations showed that the main peaks of the 2p orbitals of C1 and C2 in toluene were highly overlapping (Fig. 5e), indicating there is a strong covalent interaction between C1 and C2, leading to a higher reaction energy required for toluene ring opening. However, the corresponding covalent bonds of 2-methylbenzaldehyde are weakened (Fig. 5f), which suggests the ring opening reaction barrier of 2-methylbenzaldehyde is lower. This indicated that the ring opening reaction for 2-methylbenzaldehyde is smoother than that of toluene. Since the adsorption and activation of pollutants play a key role in thermal catalysis, the charge density differences (EDD) were calculated to investigate the interaction between the adsorbent and catalyst. The results showed that the charge of 2-methylbenzaldehyde adsorbed on the Co_3O_4 {110} facet is significantly higher than that of toluene adsorbed on the Co_3O_4 {110} facet (Fig. 5g). Therefore, the adsorption and activation of the aromatic ring of 2-methylbenzaldehyde by the catalyst are significantly stronger than those of toluene. This further verified that the co-existence of methanol could enhance the catalytic degradation of toluene in the form of complete conversion to carbon dioxide and water at a lower temperature. Moreover, the reaction barrier from methanol to formate was also calculated to estimate the effect of toluene on the catalytic oxidation of methanol (Fig. S16-17). When toluene and methanol are co-oxidized, the ΔE required for the conversion of methanol to formic acid is 0.56 eV higher than that required for the conversion of methanol to formate alone (Fig. 5h). This indicates that the presence of toluene inhibited the conversion of methanol to formate [37]. Based on these results, the reaction path for the co-oxidation of toluene and methanol is proposed as illustrated in Scheme 1. Toluene and methanol are first adsorbed on the surface of the catalyst for activation, and methanol is oxidized to formaldehyde at low temperatures. Then, the generated formaldehyde replaces the hydrogen atom in the o-position of toluene to form 2-methylbenzaldehyde. Subsequently, 2-methylbenzaldehyde is further oxidized by active oxygen species to generate 2-formaldehyde benzyl alcohol, 2-benzoic acid, etc. These species eventually react with reactive oxygen species to form maleic acid, etc., and finally carbon dioxide and water.

4. Conclusion

In summary, two Co_3O_4 catalysts with different morphologies and facets are prepared to comprehensively explore the co-oxidation and mutual-effects of vital industry VOCs of toluene and methanol. For the oxidation of single component methanol or toluene, Co_3O_4-H with a predominantly exposed {110} facet and more oxygen vacancy exhibited enhanced catalytic performance compared to Co_3O_4-N with a predominantly exposed {111} facet. Interestingly, methanol is found to promote the oxidation of toluene, leading to a significant decrease in the conversion temperature of toluene. Though the toluene slightly increases the temperature of methanol oxidation, full elimination of the mixed VOCs is unaffected by decreased energy consumption. The results of the reaction mechanism showed that the formaldehyde produced by methanol oxidation reacted with toluene to form 2-methylbenzaldehyde, which is the key to the increased the activity of toluene. This can be attributed to that the ring-opening energy barrier of 2-methylbenzaldehyde is lower than that of toluene. In addition, due to the competitive adsorption between methanol and toluene during the reaction, the conversion of methanol to formate is inhibited, resulting in lower methanol activity. This work builds a vivid example of cooperation in rational catalyst design, in-situ experimental characterization, and deep theoretical analysis to understand complex catalytic systems with mixed VOCs. It also blazes a promising trail in developing abundant, non-

expensive, and high-efficient 3D-metal catalysts, to satisfy the urgent practical needs of multicomponent VOC elimination.

CRediT authorship contribution statement

Zheng Yin: Writing – original draft, Methodology, Investigation, Formal analysis, Data curation. **Jinping Zhong:** Writing – original draft, Methodology, Formal analysis, Data curation, Conceptualization. **Tan Li:** Validation, Software, Methodology. **Fada Feng:** Validation, Investigation. **Yikui Zeng:** Writing – original draft, Visualization, Validation, Methodology, Investigation. **Dengfeng Yan:** Visualization, Investigation. **Quanming Ren:** Visualization, Investigation. **Yuanyuan Meng:** Validation, Software, Methodology. **Tao Dong:** Visualization, Investigation. **Haibao Huang:** Writing – review & editing, Data curation, Conceptualization. **Daiqi Ye:** Writing – review & editing, Funding acquisition.

Declaration of Competing Interest

The authors declare that they have no known competing financial interests or personal relationships that could have appeared to influence the work reported in this paper.

Data Availability

The data that has been used is confidential.

Acknowledgements

This work was financially supported by the Guangdong Basic and Applied Basic Research Foundation (No. 2023A1515110752), National Key Research and Development Project of Research (No. 2017YFC0212805), the National Natural Science Foundation of China (Nos. 52100121, 82204009), and the Natural Science Foundation of Guangdong Province (No. 2021A1515011378).

Appendix A. Supporting information

Supplementary data associated with this article can be found in the online version at doi:10.1016/j.apcatb.2024.124075.

References

[1] Z. Su, W. Yang, C. Wang, S. Xiong, X. Cao, Y. Peng, W. Si, Y. Weng, M. Xue, J. Li, Roles of oxygen vacancies in the bulk and surface of CeO_2 for toluene catalytic combustion, Environ. Sci. Technol. 54 (2020) 12684–12692.
[2] M.S. Kamal, S.A. Razzak, M.M. Hossain, Catalytic oxidation of volatile organic compounds (VOCs) – a review, Atmos. Environ. 140 (2016) 117–134.
[3] Q. Wang, Y. Li, A. Serrano-Lotina, W. Han, R. Portela, R. Wang, M.A. Bañares, K. L. Yeung, Operando investigation of toluene oxidation over 1D Pt@CeO_2 derived from Pt cluster-containing MOF, J. Am. Chem. Soc. 143 (2021) 196–205.
[4] Y. Guo, M. Wen, G. Li, T. An, Recent advances in VOC elimination by catalytic oxidation technology onto various nanoparticles catalysts: a critical review, Appl. Catal. B: Environ. 281 (2021) 119447.
[5] C. He, J. Cheng, X. Zhang, M. Douthwaite, S. Pattisson, Z. Hao, Recent advances in the catalytic oxidation of volatile organic compounds: a review based on pollutant sorts and sources, Chem. Rev. 119 (2019) 4471–4568.
[6] S. Rousseau, O. Marie, P. Bazin, M. Daturi, S. Verdier, V. Harlé, Investigation of methanol oxidation over Au/catalysts using operando IR spectroscopy: determination of the active sites, intermediate/spectator species, and reaction mechanism, J. Am. Chem. Soc. 132 (2010) 10832–10841.
[7] B. Huang, C. Lei, C. Wei, G. Zeng, Chlorinated volatile organic compounds (Cl-VOCs) in environment - sources, potential human health impacts, and current remediation technologies, Environ. Int. 71 (2014) 118–138.
[8] J. Li, R. Chen, W. Cui, X.A. Dong, H. Wang, K.-H. Kim, Y. Chu, J. Sheng, Y. Sun, F. Dong, Synergistic photocatalytic decomposition of a volatile organic compound mixture: high efficiency, reaction mechanism, and long-term stability, ACS Catal. 10 (2020) 7230–7239.
[9] R. Tian, J. Lu, Z. Xu, W. Zhang, J. Liu, L. Wang, Y. Xie, Y. Zhao, X. Cao, Y. Luo, Unraveling the synergistic reaction and the deactivation mechanism for the catalytic degradation of double components of sulfur-containing VOCs over ZSM-5-based materials, Environ. Sci. Technol. 57 (2023) 1443–1455.
[10] T. Pan, H. Deng, Y. Lu, J. Ma, L. Wang, C. Zhang, H. He, Synergistic catalytic oxidation of typical volatile organic compound mixtures on Mn-based catalysts: significant promotion effect and reaction mechanism, Environ. Sci. Technol. 57 (2023) 1123–1133.
[11] E.J. Moreno-Román, J. González-Cobos, N. Guilhaume, S. Gil, Toluene and 2-propanol mixture oxidation over Mn_2O_3 catalysts: study of inhibition/promotion effects by in-situ DRIFTS, Chem. Eng. J. 470 (2023) 144114.
[12] E.J. Moreno-Román, F. Can, V. Meille, N. Guilhaume, J. González-Cobos, S. Gil, MnO_x catalysts supported on SBA-15 and MCM-41 silicas for a competitive VOCs mixture oxidation: in-situ DRIFTS investigations, Appl. Catal. B: Environ. Energy 344 (2024) 123613.
[13] Y. Zeng, J. Zhong, F. Feng, D. Ye, Y. Hu, Synergistic photothermal catalytic oxidation of methanol and toluene mixture over Co-MOFs-derived catalyst: interfacial and promotion effects, Chem. Eng. J. 485 (2024) 149720.
[14] Z. Wang, P. Ma, K. Zheng, C. Wang, Y. Liu, H. Dai, C. Wang, H.-C. Hsi, J. Deng, Size effect, mutual inhibition and oxidation mechanism of the catalytic removal of a toluene and acetone mixture over TiO_2 nanosheet-supported Pt nanocatalysts, Appl. Catal. B: Environ. 274 (2020) 118963.
[15] V.P. Santos, M.F. Pereira, J.J. Orfao, J.L. Figueiredo, Mixture effects during the oxidation of toluene, ethyl acetate and ethanol over a cryptomelane catalyst, J. Hazard. Mater. 185 (2011) 1236–1240.
[16] C. He, P. Li, J. Cheng, Z.-P. Hao, Z.-P. Xu, A Comprehensive study of deep catalytic oxidation of benzene, toluene, ethyl acetate, and their mixtures over Pd/ZSM-5 catalyst: mutual effects and kinetics, Water Air Soil Pollut. 209 (2010) 365–376.
[17] W. Jiang, Y. Yu, F. Bi, P. Sun, X. Weng, Z. Wu, Synergistic elimination of NOx and chloroaromatics on a commercial V_2O_5–WO_3/TiO_2 catalyst: byproduct analyses and the SO_2 effect, Environ. Sci. Technol. 53 (2019) 12657–12667.
[18] R. Liu, H. Wu, J. Shi, X. Xu, D. Zhao, Y.H. Ng, M. Zhang, S. Liu, H. Ding, Recent progress on catalysts for catalytic oxidation of volatile organic compounds: a review, Catal. Sci. Technol. 12 (2022) 6945–6991.
[19] C. Shan, Y. Wang, J. Li, Q. Zhao, R. Han, C. Liu, Q. Liu, Recent advances of VOCs catalytic oxidation over spinel oxides: catalyst design and reaction mechanism, Environ. Sci. Technol. 57 (2023).
[20] J. Zhong, Y. Zeng, Z. Yin, M. Zhang, D. Yan, Z. Su, P. Chen, M. Fu, D. Ye, Controllable transformation from 1D Co-MOF-74 to 3D $CoCO_3$ and Co_3O_4 with ligand recovery and tunable morphologies: the assembly process and boosting VOC degradation, J. Mater. Chem. A 9 (2021) 6890–6897.
[21] Q. Yu, C. Liu, X. Li, C. Wang, X. Wang, H. Cao, M. Zhao, G. Wu, W. Su, T. Ma, J. Zhang, H. Bao, J. Wang, B. Ding, M. He, Y. Yamauchi, X.S. Zhao, N-doping activated defective Co_3O_4 as an efficient catalyst for low-temperature methane oxidation, Appl. Catal. B: Environ. 269 (2020) 118757.
[22] Z. Xiao, Y.-C. Huang, C.-L. Dong, C. Xie, Z. Liu, S. Du, W. Chen, D. Yan, L. Tao, Z. Shu, G. Zhang, H. Duan, Y. Wang, Y. Zou, R. Chen, S. Wang, Operando identification of the dynamic behavior of oxygen vacancy-rich Co_3O_4 for oxygen evolution reaction, J. Am. Chem. Soc. 142 (2020) 12087–12095.
[23] Y. Jian, M. Tian, C. He, J. Xiong, Z. Jiang, H. Jin, L. Zheng, R. Albilali, J.-W. Shi, Efficient propane low-temperature destruction by Co_3O_4 crystal facets engineering: unveiling the decisive role of lattice and oxygen defects and surface acid-base pairs, Appl. Catal. B: Environ. 283 (2021) 119657.
[24] J. Zhong, Y. Zeng, M. Zhang, W. Feng, D. Xiao, J. Wu, P. Chen, M. Fu, D. Ye, Toluene oxidation process and proper mechanism over Co_3O_4 nanotubes: investigation through in-situ DRIFTS combined with PTR-TOF-MS and quasi in-situ XPS, Chem. Eng. J. 397 (2020) 125375.
[25] S. Mo, Q. Zhang, J. Li, Y. Sun, Q. Ren, S. Zou, Q. Zhang, J. Lu, M. Fu, D. Mo, J. Wu, H. Huang, D. Ye, Highly efficient mesoporous MnO_2 catalysts for the total toluene oxidation: oxygen-vacancy defect engineering and involved intermediates using in situ DRIFTS, Appl. Catal. B: Environ. 264 (2020) 118464.
[26] C. Dong, Z. Qu, Y. Qin, Q. Fu, H. Sun, X. Duan, Revealing the highly catalytic performance of spinel $CoMn_2O_4$ for toluene oxidation: involvement and replenishment of oxygen species using in situ designed-TP techniques, ACS Catal. 9 (2019) 6698–6710.
[27] J. Li, H. Na, X. Zeng, T. Zhu, Z. Liu, In situ DRIFTS investigation for the oxidation of toluene by ozone over Mn/HZSM-5, Ag/HZSM-5 and Mn–Ag/HZSM-5 catalysts, Appl. Surf. Sci. 311 (2014) 690–696.
[28] Z. Xie, J. Zhong, J. Tian, P. Liu, Q. Ren, L. Chen, M. Fu, D. Ye, Unraveling the role of OH groups over CeO_2 derived from methanol modification for enhancing toluene oxidation: experimental and theoretical studies, Appl. Catal. A: Gen. 654 (2023) 119069.
[29] B. Kortewille, I.E. Wachs, N. Cibura, O. Pfingsten, G. Bacher, M. Muhler, J. Strunk, Photocatalytic methanol oxidation by supported vanadium oxide species: influence of support and degree of oligomerization, Eur. J. Inorg. Chem. 2018 (2018) 3725–3735.
[30] L.J. Burcham, M. Badlani, I.E. Wachs, The origin of the ligand effect in metal oxide catalysts: novel fixed-bed in situ infrared and kinetic studies during methanol oxidation, J. Catal. 203 (2001) 104–121.
[31] S.D. Lin, H. Cheng, T.C. Hsiao, In situ DRIFTS study on the methanol oxidation by lattice oxygen over Cu/ZnO catalyst, J. Mol. Catal. A: Chem. 342-343 (2011) 35–40.
[32] M.V. Bosco, M.A. Bañares, M.V. Martínez-Huerta, A.L. Bonivardi, S.E. Collins, In situ FTIR and Raman study on the distribution and reactivity of surface vanadia species in V_2O_5/CeO_2 catalysts, J. Mol. Catal. A: Chem. 408 (2015) 75–84.
[33] Y. Zeng, J. Zhong, H. Wang, M. Fu, D. Ye, Y. Hu, Synergistic effect of tunable oxygen-vacancy defects and graphene on accelerating the photothermal degradation of methanol over Co_3O_4/rGO nanocomposites, Chem. Eng. J. 425 (2021) 131658.

[34] R.S. Blake, K.P. Wyche, A.M. Ellis, P.S. Monks, Chemical ionization reaction time-of-flight mass spectrometry: multi-reagent analysis for determination of trace gas composition, Int. J. Mass Spectrom. 254 (2006) 85–93.
[35] J. Zhong, Y. Zeng, D. Chen, S. Mo, M. Zhang, M. Fu, J. Wu, Z. Su, P. Chen, D. Ye, Toluene oxidation over Co^{3+}-rich spinel Co_3O_4: evaluation of chemical and by-product species identified by in situ DRIFTS combined with PTR-TOF-MS, J. Hazard. Mater. 386 (2020) 121957.
[36] B. Chen, B. Wu, L. Yu, M. Crocker, C. Shi, Investigation into the catalytic roles of various oxygen species over different crystal phases of MnO_2 for C_6H_6 and HCHO oxidation, ACS Catal. 10 (2020) 6176–6187.
[37] J. Wang, G. Zhang, J. Zhu, X. Zhang, F. Ding, A. Zhang, X. Guo, C. Song, CO_2 hydrogenation to methanol over In_2O_3-based catalysts: from mechanism to catalyst development, ACS Catal. (2021) 1406–1423.